Journal of Polymers and the Environment (2024) 32:3342–3362
https://doi.org/10.1007/s10924-023-03163-8

ORIGINAL PAPER

Melt-Extruded Home Compostable Films Based On Blends Of Thermoplastic Gliadins And Poly(ε-Caprolactone) Intended For Food Packaging Applications

Alejandro Aragón-Gutiérrez[1] · Pedro Francisco Muñoz-Gimena[2] · Miriam Gallur[1] · Rafael Gavara[3,4] · Daniel López[2,4] · Pilar Hernández-Muñoz[3,4]

Accepted: 12 December 2023 / Published online: 23 January 2024

Abstract
Biodegradable polymers for food applications have emerged as a sustainable alternative to reduce plastic waste. In this work, compostable films based on blends of poly(ε-caprolactone) (PCL) and thermoplastic gliadins (TPG) were developed for packaging applications. Firstly, gliadins were extracted from wheat gluten and plasticized with glycerol. Then, PCL/TPG films were prepared by cast-extrusion processing at pilot scale and samples were characterized in terms of their structural, morphological, thermal, mechanical, barrier and optical properties. The addition of TPG increased the glass transition temperature (T_g) of PCL, reduced the oxygen permeability at 0% and 50% relative humidity values, and improved the seal strength properties of the films, having a minimal effect on the thermal stability, transparency, and the high stretchability characteristic of PCL. On the other hand, the presence of gliadins led to more water sensitive materials, resulting in a slight increase in the water vapor permeability. Finally, the home-compostability assessment of the films revealed that the presence of gliadins accelerated the aerobic biodegradation and the disintegration with respect to pristine PCL film, thus, showing the potential interest of the developed materials for sustainable packaging applications.

✉ Alejandro Aragón-Gutiérrez
alejandro.aragon@itene.com

[1] Grupo de Tecnología de Materiales y Envases, Instituto Tecnológico del Embalaje, Transporte y Logística, ITENE, Unidad Asociada Al CSIC, Calle de Albert Einstein 1, 46980 Paterna, Valencia, Spain

[2] Instituto de Ciencia y Tecnología de Polímeros, ICTP-CSIC, Calle Juan de La Cierva 3, 28006 Madrid, Spain

[3] Instituto de Agroquímica y Tecnología de Alimentos, IATA-CSIC, Calle del Catedrático Agustín Escardino Benlloch 7, 46980 Paterna, Valencia, Spain

[4] Interdisciplinary Platform for "Sustainable Plastics Towards a Circular Economy" (SusPlast-CSIC), 28006 Madrid, Spain

Graphical Abstract

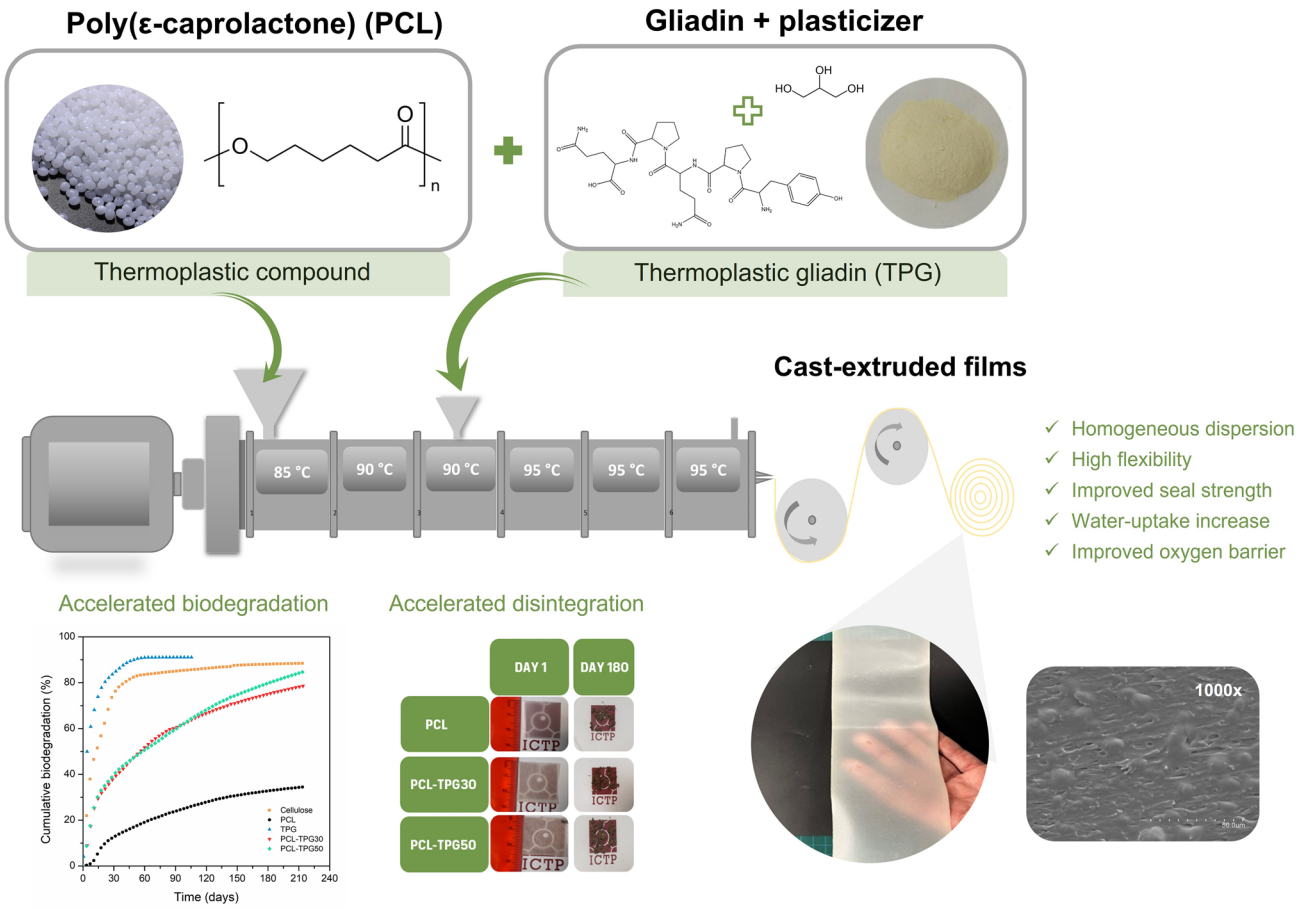

Keywords Poly(ε-caprolactone) · Thermoplastic gliadins · Extrusion · Polymer blends · Film properties · Compostability · Sustainable food packaging

Introduction

The use of non-biodegradable polymers derived from petrochemical resources to manufacture short-term or single-use plastic products (e.g., food packaging) has been revealed as a serious environmental concern in the last years [1]. Specifically, packaging applications represent the largest sector with around 30 % of total plastic consumption worldwide, and of that quantity, ca. 45 % is used for single-use packaging [2–4]. Therefore, current trends and efforts in food packaging science and technology are mainly focused on substituting non-biodegradable materials by biodegradable and compostable ones. Currently, it is already possible to find a wide list of compostable plastics available in the market including polylactic acid (PLA), polyhydroxyalkanoates (PHAs), poly(ε-caprolactone) (PCL), polybutylene succinate (PBS) or polybutyleneadipate-co-terephthalate (PBAT) [5–7]. Among these polymers, PCL has gained great attention in recent years due to its great stretchability, low glass transition temperature, $T_g = -60$ °C, and good miscibility and compatibility with other polymers [8]. In addition, PCL can decompose into carbon dioxide, methane, water, inorganic compounds, and biomass by the enzymatic action of both, aerobic and anaerobic microorganisms [9]. However, PCL also has some drawbacks. Firstly, commercial PCL is not considered biobased since it is synthesized through the ring-opening polymerization of ε-caprolactone in the presence of a catalyst and a macroinitiator. On the other hand, the low melting point (60-65 °C) of PCL restricts its use in many applications and processes that have high temperature requirements, and, finally, the manufacturing process of PCL is complex and expensive with market prices above 14 €/kg, thus, limiting its application in food packaging [10, 11]. With this in mind, blending polycaprolactone with food hydrocolloid matrixes such as carbohydrate polymers (e.g., starch and chitosan) or proteins has been

positioned as an encouraging strategy to enhance PCL properties and reduce its price. Starch has been the preferable option for preparing PCL-based blend films. For example, Avella et al. prepared blends of PCL with 45 % of starch, resulting in fully biodegradable materials with enhanced biodegradation rate thanks to the presence of starch [12]. Ramirez-Arreola and coworkers studied the influence of PCL concentration on the functional properties and blow-up ratio of PCL-thermoplastic starch blown films [13]. It is also possible to find commercial grades consisting of PCL/starch blends under the trade names Mater-Bi^{TM} and Envar supplied, respectively, by Novamont (Italy) and BioPlastics Inc. (The Netherlands). With respect to PCL/protein blends, Corradini et al. prepared polycaprolactone/zein sheets at diverse concentrations by compression molding and studied their mechanical and thermal performance, showing that the thermal stability and the elongation at break decreased as the content of zein in the blend increased [14]. Several works also report the development of blends of PCL and wheat gluten. John et al. extruded PCL and PCL-grafted with maleic anhydride (MA) with different amounts of wheat gluten and concluded that the presence of MA improved the interaction between PCL and wheat gluten, thus, resulting in a better mechanical performance [15]. Finkenstadt and coworkers used a pilot-scale twin-screw extruder to obtain biodegradable PCL-based films incorporating up to 50 % w/w of wheat gluten [16]. More recently, Gutiérrez et al. developed films by extrusion followed by thermo-molding consisting of crosslinked blends of PCL and thermoplastic gluten by the action of chrome octanoate as catalyst. They showed that the incorporation of the catalyst resulted in more crystalline materials with better water-resistant properties whereas the compostability was not significantly affected by the crosslinking [17]. These works showed promising alternatives to enhance the performance of PCL, increase the renewable and bio-based content of material in the formulation and make the PCL-based plastic more cost-effective. Some research works on gluten proteins have also established that the two components comprising gluten, gliadin and glutenin, can be used individually to expand their range of applications [18]. Following this approach, in the present study, gliadins, the major component of wheat gluten, were selected due to their easy extractability in alcoholic solutions and great film-forming capacity, to obtain a thermoplastic gliadin (TPG) resin for its further use in the development of blends of PCL and TPG by a conventional film-extrusion transformation process.

Therefore, the overall objective of this research was to prepare and ascertain the performance of compostable films based on PCL blended with 30 wt. % and 50 wt. % of thermoplastic gliadins. To this aim, gliadins were extracted from wheat gluten and plasticized with glycerol in order to improve their processability by melt-extrusion. Then, films of PCL and TPG were obtained in a pilot-scale extruder and characterized by means of structural, morphological, thermal, mechanical, optical and barrier properties aiming to determine their suitability for food applications. Finally, the compostability of the films was assessed to determine the influence of gliadins on the biodegradation and disintegration rate of PCL under home-composting conditions.

Materials and Methods

Materials

Poly(ε-caprolactone) (Capa^{TM} 6500, Ingevity) was supplied by Ravago Chemicals Spain S.A. (Barcelona, Spain). Wheat gluten was provided by VicorQuimia S.A. (Badalona, Barcelona, Spain). Glycerol, ethanol, and microcrystalline cellulose (particle diameter around 20 µm) were purchased from Sigma-Aldrich Química S.A. (Madrid, Spain). Water was obtained from an ultrapure water system Barnstead GenPure Pro (Thermo Fischer Scientific, Massachusetts, MA, USA).

Gliadin-Rich Fraction Extraction from Wheat Gluten and Plasticization

The gliadin fraction was extracted from wheat gluten following the method reported by Balaguer et al. [19]. In brief, 1 kg of wheat gluten was dispersed in 4 L of 70 % (v/v) ethanol/water mixture and stirred vigorously at room temperature overnight. The gliadin-rich fraction was recovered by using a pressure filter pocket (ICT Filtration S.L., Barcelona, Spain). Then, the solid content of the solution was determined, and glycerol was added in 25 wt. % with respect to the gliadin fraction. Finally, the solvent was allowed to evaporate, and the final material was powdered using a cutting mill SM 2000 (Retsch GmbH, Haan, Germany).

Preparation of Films Based on PCL-Gliadin Blends by Extrusion Processing

Blend films of PCL, and PCL incorporating 30 wt. % (PCL-TPG30) and 50 wt. % (PCL-TPG50) of plasticized gliadins were prepared in a pilot scale co-rotating twin-screw extruder Brabender TSE 20/40 with a 20 mm diameter screw and a length-diameter ratio (L/D) of 40. PCL pellets were fed through the main hopper employing a gravimetric feeder (MGF-3-ST, MAGUIRE, Staffordshire, United Kingdom) while plasticized gliadins in powder form were introduced downstream of the extruder by using a side volumetric feeder. The screw speed was set at 35 rpm, and the operating temperature were, from hopper to die, 85-90-90-95-95-95 °C. Films, around 8 cm in width and thicknesses in the range of 160-220 µm were obtained using an extrusion

roller calender line and stored in multilayer PET/Aluminum/LDPE bags.

Characterization of Melt-Extruded Compostable Films

Fourier Transform Infrared Spectroscopy (FTIR)

FTIR analysis in attenuated total reflection mode was carried out using a TENSOR 27 Spectrophotometer (Bruker, Massachusetts, USA) coupled to a diamond ATR Golden Gate™ Specac accessory (Teknokroma, Barcelona). Spectra were recorded in the range of 4000-700 cm^{-1}, averaging 32 scans at a resolution of 4 cm^{-1}.

Morphological and Structural Characterization.

The microstructural evaluation of the cross sections of the films was carried out by scanning electron microscopy (SEM-FEG Hitachi S-4800, Hitachi Ltd, Tokyo, Japan) using an accelerating voltage of 10 kV and a working distance of 12 mm. Films were cut crosswise with a crioultramicrotome and the cross areas were coated with a thin layer of Au/Pd prior to the analysis to increase their conductivity. The particle/agglomerate size of gliadins in PCL-TPG blends was analyzed using ImageJ software.

The crystalline structural characterization was examined with a D8 ADVANCE A25 X-ray diffractometer (Bruker, Massachusetts, MA, USA). The XRD patterns were obtained by using Cu/K_α radiation, in the angle range from 2° to 60°, at a scan speed of 2°/min with a collection time of 0.2 s per step.

Thermal Properties: Thermogravimetric Analysis (TGA) and Differential Scanning Calorimetry (DSC).

The thermal stability of plasticized gliadins and PCL-based formulations was evaluated by thermogravimetric analysis by using a TGA Q-500 instrument (TA Instruments, New Castle, DE, USA) under nitrogen flow at a constant heating rate of 10 °C min^{-1} from room temperature to 900 °C. DSC analysis was carried out using a DSC Q-2000 calorimeter and consisted of a heating scan from −90 to 140 °C, followed by a cooling from 140 to −90 °C and a final heating scan −90 to 140 °C. The scans were carried out under constant nitrogen flow and the heating and cooling rates were 10 °C min^{-1}. The melting point, the crystallization temperature and their corresponding enthalpies were determined using the TA Universal Analysis Software. The crystallinity degree of PCL in all samples was calculated following Equation 1

$$X_c(\%) = \frac{\Delta H_m}{\Delta H_m^0} x \frac{1}{w_f} x100 \quad (1)$$

where ΔH_m is the melting enthalpy of the sample during the first heating scan, ΔH_m^0 is the melting enthalpy for a 100% crystalline PCL (139.5 J g^{-1})[20], and w_f is the weight fraction of PCL in the blend.

Dynamic Mechanical Thermal Analysis

Dynamical mechanical thermal analysis (DMTA) was carried out using a DMA/SDTA861e analyzer (Mettler-Toledo, Ohio, OH, USA) in clamp tension mode. An amplitude of 15 µm was kept constant, and analyses were conducted at a frequency of 1, 3, 10, 30 Hz, and a normal force of ±2 N was set. The temperature was monitored between −120 °C and 50 °C range at a heating rate of 2 °C min^{-1}. Samples had approximate dimensions of 11, 5 and 0.2 mm in length, width, and thickness, respectively.

Mechanical Properties and Seal Strength

Tensile testing of films was conducted using a universal testing machine Testometric M350-20CT (Rochdale, UK), equipped with a 100 N load cell. Tests were carried out in accordance with the standard ISO 527-3 [21], and the films with dimensions of 100 mm length, 15 mm width and an average thickness around 0.2 mm, were stretched at a test speed of 100 mm min^{-1}. Young Modulus (E), stress at yield (σ_y), stress at break (σ_B) and elongation at break (ε_B) were determined from the stress-strain curves as the average of at least five measurements. The seal strength of the films was evaluated according to ASTM F88/F88M-15 [22]. The films were sealed using a pressure of 0.2 MPa, a sealing time of 1 second and the temperature was varied in the range of 60 to 65 °C. Then, heat-sealed rectangular samples with a size of 40 x 15 mm were prepared. Finally, the unsealed edges of the films were fixed to the tension test clips of the Universal testing machine and subjected to an extension velocity of 200 mm min^{-1}. The seal strength was calculated as the average between 20 % and 80 % displacement, as reported in the standard, following Equation 2

$$Seal\ strength = \frac{Mean\ Force(N)}{Film\ width(mm)} \quad (2)$$

Water Uptake and Water Contact Angle Measurements.

The water absorption capacity of the developed films was determined following the method reported by Kormin and coworkers [23]. In brief, film samples with sizes around 3 x 3 cm were dehydrated by storing them for two weeks in

desiccators containing silica gel. After that period, a water content close to zero was assumed, and the initial weight (W_i) of the samples was recorded. Then, samples were immersed in tubes containing distilled water for 24 hours. Finally, films were recovered from the tubes, and the excess of water was eliminated from the surface of the samples with absorbent paper before determining their final weight (W_f). The percentage water uptake (WU %) was calculated using the following formula:

$$Water\ uptake\ (\%) = \frac{W_f - W_i}{W_i} x100 \quad (3)$$

Surface wettability was determined by water contact angle measurements at room temperature employing a goniometer OCA 15EC (Dataphysics, Germany). A drop of water of 5 µL was placed on each film surface at random positions and the contact angles were recorded for 60 seconds. A minimum of 5 measurements were carried out of each reference.

Barrier Properties: Oxygen and Water Barrier Permeability Coefficients.

The oxygen permeability coefficients of PCL and PCL/TPG films were determined employing an OX-TRAN Model 2/22 H OTR Analyzer Mocon (Lippke, Neuwied, Germany). Tests were carried out at room temperature and at three different relative humidity values (RH): 0 %, 50 % and 75 % RH in accordance with ASTM D3985-17 (dry conditions) and F1927-20 (controlled humidity conditions) [24, 25]. Water vapor permeability was evaluated following the ASTM F1249-20 [26], at room temperature and 50 % RH, using a Permatran-W Model 3/34 G.

Colour Properties

The color coordinates in the CIELab space: L^* (lightness), a^* (red-green), b^* (yellow-blue), were evaluated using a KONICA CM-2500d instrument (Konica Minolta Sensing Americas, Inc., NJ, USA). The color difference (ΔE) of PCL-TPG films with respect to the control PCL film was determined following Equation 4

$$\Delta E = [(\Delta L)^2 + (\Delta a^*)^2 + \left(\Delta b^*\right)^2]^{0.5} \quad (4)$$

Home-Compostability Assessment

Aerobic Biodegradation The aerobic biodegradability of the materials under controlled composting conditions was determined by measuring the amount of evolved carbon dioxide (CO_2) following the standards NF T 51-800 and ISO 14855-1:2012 [27, 28]. The inoculum was prepared by mixing 200 grams of well aerated compost from a working composting plant with 50 grams of vermiculite (ratio compost: vermiculite of 4:1). Distilled water was added to achieve a moisture content over 40 %. Then, 250 grams of this mixture was placed in a 2-L glass flask (bioreactor) with a lower inlet for H_2O-saturated air and an upper outlet for the analysis of CO_2 in a non-dispersive infrared equipment (LI-830 CO_2 analyzer, LI-COR Biosciences GmbH). The aerobic conditions during the test were maintained thanks to an air compressor that supplied dry air to the system and to a flow regulation system. Once prepared, 15 grams of test sample was added in the form of powder (plasticized gliadins) or pellet (PCL, PCL-TPG-30 and PCL-TPG50). In addition, one bioreactor containing microcrystalline cellulose mixed with the compost was used as reference sample while another bioreactor with the compost alone, i.e., without addition of an external carbon source, was used as a blank. Tests were carried out in triplicate and the reactors were placed in a hot air oven (Dry-big 720 L, J.P. Selecta, Spain) operating at 25 ± 5 °C throughout the test.

The theoretical amount of carbon dioxide ($ThCO_2$) that can be produced by the test material in each bioreactor assuming that all the organic carbon of the sample is converted into CO_2, was calculated using the following Equation

$$ThCO_2 = W_s x C_T x \frac{MW_{CO2}}{MW_C} \quad (5)$$

where W_s is the dry weight in grams of the test sample introduced in the bioreactor, C_T is the proportion of the total organic carbon in the dry sample (grams of C/ grams of dry sample) and MW_{CO2} and MW_C are, respectively, the molecular weights of carbon dioxide (44 g/mol) and carbon (12 g/mol). The percentage of biodegradation (%B) was determined from the cumulative amount of CO_2 generated, by using the following Equation

$$B(\%) = 100x\frac{\sum CO_{2S} - \sum CO_{2B}}{ThCO_2} \quad (6)$$

where $\sum CO_{2S}$ is the cumulative amount of CO_2 (g) generated in the bioreactor containing the test sample, $\sum CO_{2B}$ is the cumulative amount of CO_2 (g) produced in the blank bioreactor, and $ThCO_2$ is the previously calculated theoretical amount of CO_2 that can be produced by the test material.

2.4.1.2. Disintegration under home-composting conditions.

The evaluation of disintegrability of PCL and PCL-TPG films was conducted via weight loss determination after their burial in compost. The dried film samples were cut into 2.5 × 2.5 cm^2, and the initial weight (M_0) of each film was recorded. Afterward, the samples were placed in textile meshes buried in synthetic wet compost and subjected to an aerobic disintegration process for 180 days. Composting test

was carried out at 25 °C under home composting conditions in accordance with the French standard NF T 51-800 [27]. The synthetic wet compost was prepared by mixing 45 wt. % of solid synthetic wet waste [10% of compost (COMPO EXPERT S.L., Spain), 30 % rabbit food, 10 % starch, 5 % sugar, 4 % corn oil, 1 % urea, and 40 % sawdust] and 55 wt. % of water contained in a perforated plastic box as composter reactor following the ISO 20200 standard [29]. During the incubation, water was sprayed on the compost surface and periodically mixed to avoid moisture loss. Each film sample was taken out from the compost soil after 1, 4, 19, 31, 71, 120 and 180 days of incubation, cleaned with a brush to remove the adhered compost and weighted (M_t) after drying in an oven in soft conditions. Finally, the percentage of disintegrability of PCL and PCL-TPG films was calculated according to the following Equation:

$$Disintegrability\,(\%) = \left(\frac{M_0 - M_t}{M_0}\right) x100 \quad (7)$$

Results

Development of Cast-Extruded Films Based on PCL and TPG

Supplementary Figure S1 illustrates the setup of the extrusion process used to produce various references through melt-blending at a pilot scale.. The processing conditions were kept constant for the three references in terms of temperature profile and screw rotation speed (85–90-90–95-95–95 °C and 35 rpm, respectively). However, it was possible to observe in the plastogram that the torque profile of the extruder increased with the incorporation of plasticized gliadins, shifting from an average value of 35 N·m to 43.4 N·m and 45.9 N·m in PCL-TPG30 and PCL-TPG50 blends, respectively. This noticeable increase in the torque was attributed, on the one hand, to the viscous nature of gliadins and on the other hand, to potential crosslinking reactions of protein chains promoted by the shear stresses and the relatively high temperatures during the extrusion process, as suggested in previous works [30, 31]. As a consequence, the roll speed of the calender line was adjusted for each formulation to obtain films with thickness in the range of 160–220 µm. FTIR analysis .

FTIR spectroscopy analysis was carried out to identify the functional groups present in the prepared films or to detect the formation of new bonds as a result of interactions between PCL and gliadins. The spectra of the neat gliadin, PCL and PCL-TPG blends are shown in Figure 1. Thermoplastic gliadin exhibited the characteristic stretching bands of free amino groups and water in the wavenumber range of 3500-3100 cm^{-1} and the three characteristic absorption peaks associated with the amide I band at 1634 cm^{-1}, the bending vibration of N−H (amide II) at 1536 cm^{-1} and the amide III at 1444 cm^{-1} [32]. On the other hand, neat PCL showed bands at 2944 and 2865 cm^{-1}, attributed to the symmetric and asymmetric stretching vibration of C−H_2, the prominent peak at 1720 cm^{-1} was related to the stretching vibration of the C=O carbonyl group and the peaks at 1294 and 1162 cm^{-1} were assigned to the asymmetric and

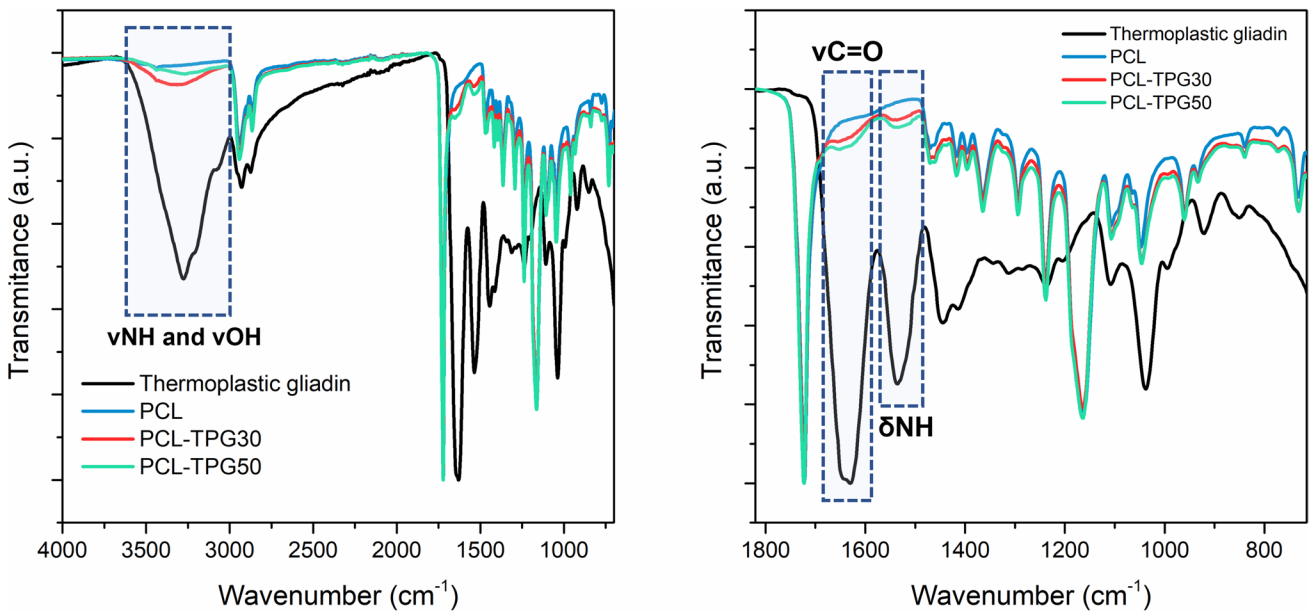

Fig. 1 FTIR-ATR spectra of PCL, thermoplastic gliadin, and binary blend films

symmetric stretching vibrations of C−C and C−O−C [33, 34]. By the melt mixing process of gliadins with PCL, no new bands were detected in the FTIR spectra. However, the appearance of weak peaks in PCL-TPG30 and PCL-TPG50 assigned to the stretching vibration of N−H and O−H, the stretching vibration of C=O bond of the amide I and the bending vibration of N−H of the amide II in gliadins, confirmed the successful physical blending of both components.

Microstructural Analysis

Figure 2 shows the micrographs of the cross area of films subjected to cryofracture obtained by SEM observation. As expected, pristine PCL sample presented a smooth, homogeneous, and continuous phase, with a fracture pattern that can be related to a ductile behavior. The same observations on PCL films have been made in previous works [35, 36]. On the contrary, the incorporation of plasticized gliadins resulted in heterogeneities along the cross sections of the films, which were more evident as the content of gliadins increased in the sample. The observation of random-order conglomerates of gliadins in the binary blends, with a particle size between 1 and 25 µm (Suppl. Figure S2), suggested a lack of miscibility of both components [37]. However, no discontinuities in the form of micro-pores or voids indicated that the polymer flow during the melt-blending process was appropriate with the used conditions [38].

XRD Analysis

X-ray diffraction analysis was conducted to investigate the crystalline structure of the formulations under study. The XRD patterns of thermoplastic gliadin, neat PCL, and PCL-TPG blends (Suppl. Figure S3), along with a detailed discussion of the results, can be found in the Supporting Information section.

Thermal Analysis

Figure 3 presents the DSC heating and cooling thermograms of PCL and PCL-plasticized gliadins binary blends and * MERGEFORMAT Table 1 shows the main thermal parameters obtained from these curves. The degree of crystallinity of the three formulations was determined from the first heating scan of the DSC analysis. Gliadins are individual protein molecules composed of amino acid chains linked by inter-chain disulfide bonds and their transition from a glassy to a rubbery state is highly dependent on the moisture or plasticizer content [15, 32]. Pure dehydrated gliadins presented a glass transition temperature (T_g) of 160 °C while the addition of 25 % w/w of glycerol lowered their T_g to 90 °C,

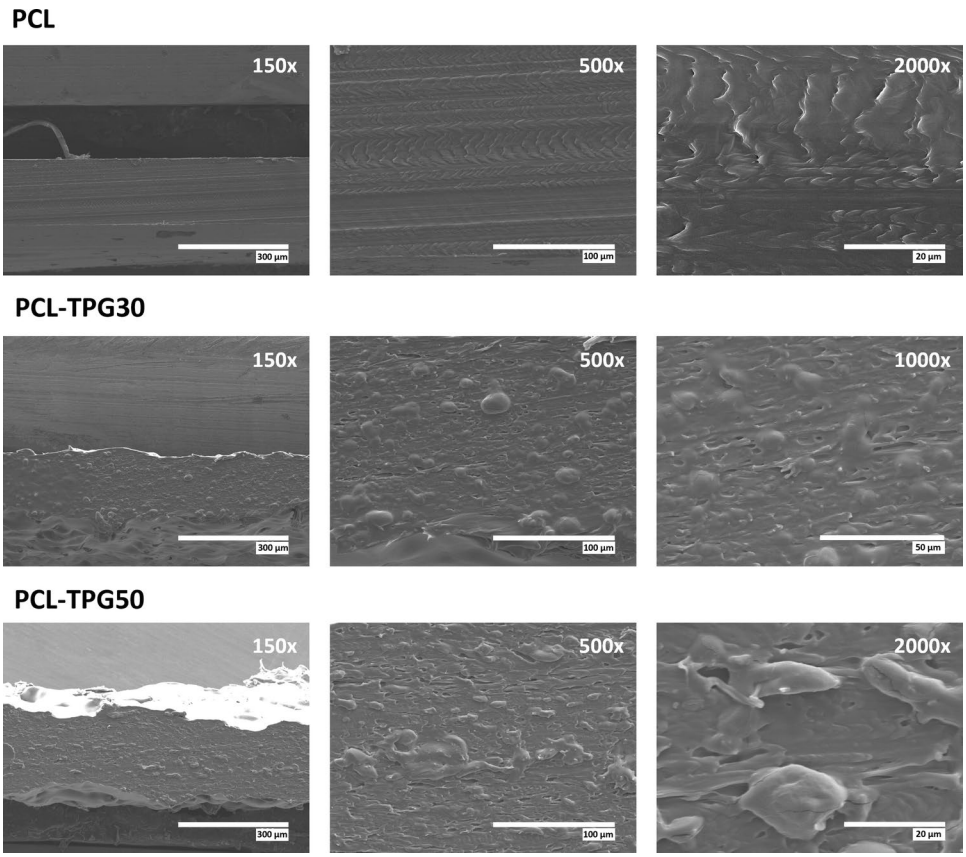

Fig. 2 SEM micrographs of cross-sectional areas of PCL, PCL-TPG30 and PCL-TPG50 films at different magnifications

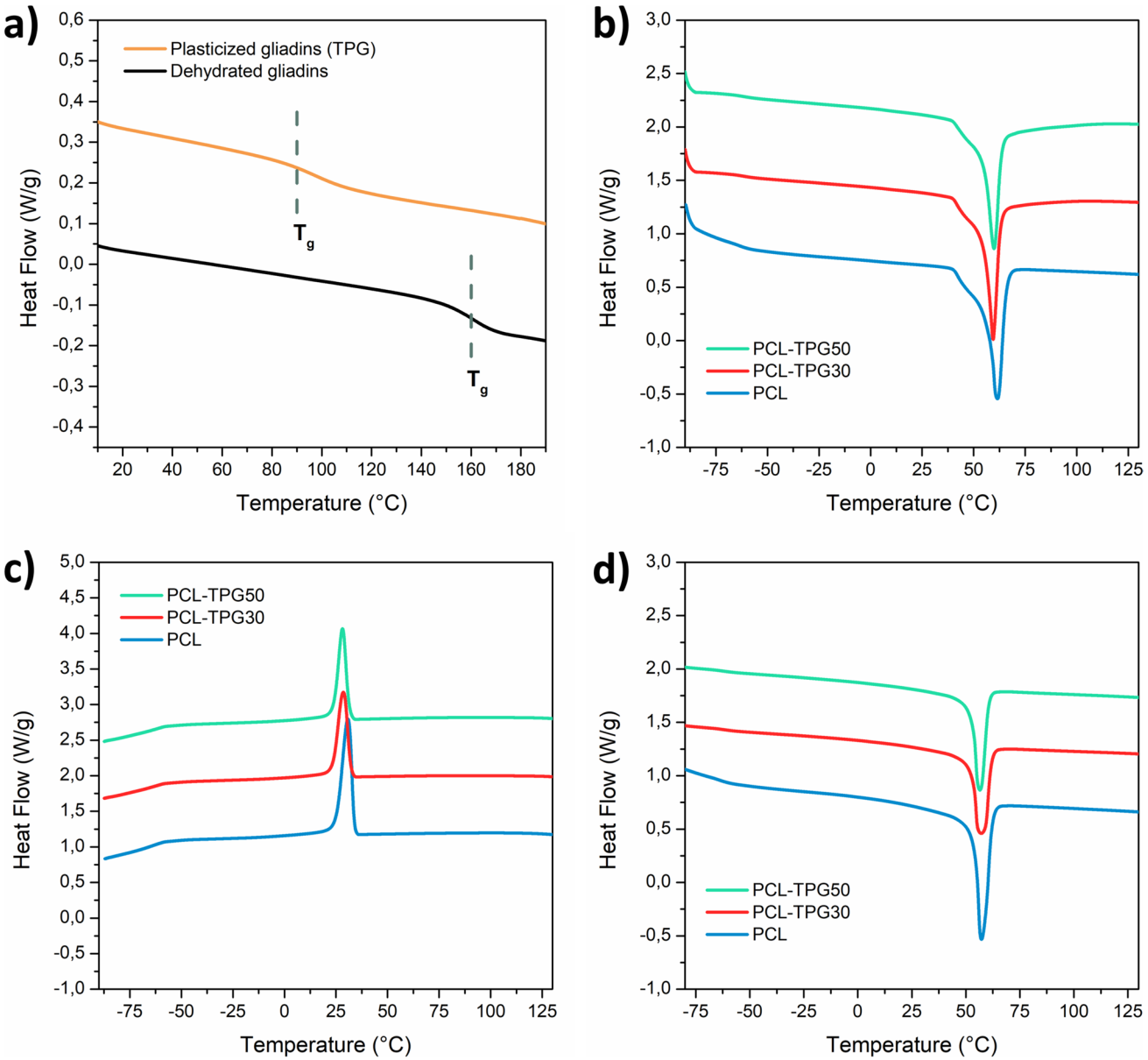

Fig. 3 DSC thermograms of PCL, gliadin and the binary PCL/TPG blends: gliadins, second heating (**a**), PCL and blends, first heating (**b**), cooling (**c**) and second heating scan (**d**)

Table 1 DSC thermal parameters and crystallinity degree of PCL, and PCL/TPG blends

	First heating scan			Cooling scan		Second heating scan	
Reference	T_m (°C)	ΔH_m (J/g)	X_c (%)	T_c (°C)	ΔH_c (J/g)	T_m (°C)	ΔH_m (J/g)
PCL	61	79.7	57.1	31	58.2	57	59.7
PCL-TPG30	59	64.1	65.6	29	43.4	57	40.8
PCL-TPG50	59	58.0	83.1	27	37.9	56	37.5

X_c, degree of crystallinity (%) calculated during the first heating scan

being in good agreement with the data reported in previous works [39, 40]. The thermogram of neat PCL showed, during the first and second heating scans, endothermic peaks at 61 °C and 57 °C, respectively, which is in accordance with the typical values of the melting point of PCL, whereas during the cooling scan, the crystallization peak temperature

was located at 31 °C [41]. A small shoulder prior to the melting peak was observed in the first heating scan, attributed to heterogeneous crystal size populations. This phenomenon can be explained by the sudden cooling from the molten state to the roll temperature −2 °C− when the samples were processed by film-extrusion. In the case of PCL-TPG (70/30 and 50/50) blends, the incorporation of gliadins did not induce an evident change in the melting point with respect to pristine PCL. However, the crystallinity degree of PCL-TPG blends, obtained after normalizing the actual PCL amount in the blend (calculated from the first heating thermogram), increased significantly by the incorporation of plasticized gliadins from 57.1 % for PCL to 65.6 % and 83.1 % for PCL-TPG30 and PCL-TPG50, respectively, indicating that gliadins promoted an evident nucleating effect on the PCL polymer matrix. In addition to this, a slight decrease in the PCL crystallization temperature (T_c) from 31 °C to 29 and 27 °C in PCL-TPG30 and PCL-TPG50, respectively, was observed in the film formulations. This result was related to a heterogenous nucleation of PCL induced by the presence of gliadins, thus, obtaining lower T_c values [42, 43].

Figure 4 shows the TGA thermograms of the PCL, the thermoplastic gliadin, and the binary mixtures of PCL/TPG while Table 2 reports the main thermal parameters determined from the TGA and DTG (first derivative) curves. PCL showed a great thermal stability, presenting an onset degradation temperature calculated at a 5 % weight loss of 369 °C. Then, a single stage degradation temperature was observed, with a maximum decomposition temperature centered at 408 °C. However, some works have reported that the degradation process of PCL consists of a two-stage process: first, a polymer chain cleavage via cis-elimination reaction, and then, the unzipping depolymerization from the PCL chain's −OH end groups [44, 45]. On the other hand, plasticized gliadins presented an T_{onset} of 112 °C. The weight loss in the range from 30 to 220 °C was attributed to the desorption of water and to the loss of low molecular weight components, i.e., glycerol [38]. Then, the destruction of gliadin structure, including the cleavage of S−S, O−N, and O−O linkages of protein molecules, occurred in the range of 260 °C and 395 °C, with a maximum peak temperature located at 312 °C [46]. Regarding the binary systems of PCL/TPG, the incorporation of gliadins into the PCL matrix led to a noticeable shift in the onset degradation temperature ($T_{5\%}$) of PCL towards lower values as the content of TPG in the films increased. This decrease in the $T_{5\%}$ was related to the previously mentioned water content and the loss of low molecular weight components in the samples. Positively, the onset degradation temperatures were found to be significantly higher than the processing temperature of the films,

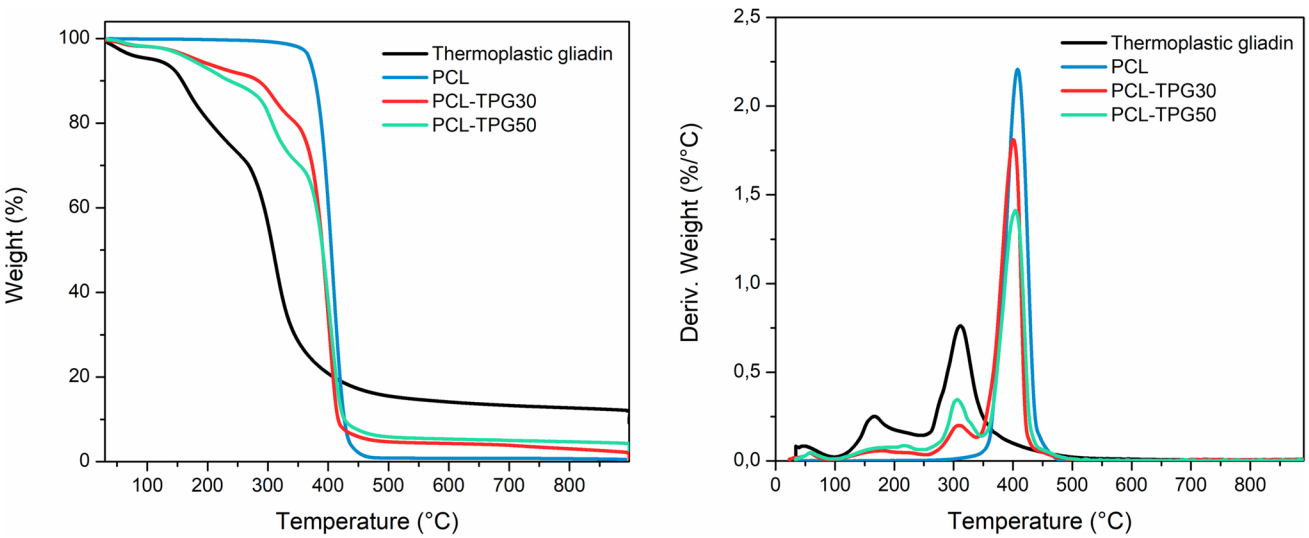

Fig. 4 TGA (left) and DTG (right) curves of PCL, gliadin and the binary PCL/TPG blends

Table 2 Onset degradation temperature and maximum degradation temperatures of PCL and PCL/TPG blends

Reference	$T_{5\%}$ (°C)	$T_{max,\ I}$ (°C)	$T_{max,\ II}$ (°C)	$T_{max,\ III}$ (°C)	$T_{70\%}$(°C)	Residue (%)
TPG	112	165	312	–	344	11.96
PCL	369	–	–	408	414	0.57
PCL-TPG30	182	167	305	401	402	2.23
PCL-TPG50	173	168	306	403	405	4.27

ensuring the structural integrity of the formulations during the manufacturing process. This thermal stability suggested that the PCL/TPG binary systems are well-suited for melt-extrusion processing techniques. Upon analyzing the DTG curves of the binary blends, three main degradation stages could be observed. Firstly, a broad and low intensity peak from 120 to 260 °C was related to the loss of the glycerol used as gliadin-plasticizer. Secondly, between 255 and 350 °C, a peak temperature associated with the degradation of the principal structure of gliadin was detected. Finally, a sharp peak around 401-403 °C was observed, whose intensity decreased as the content of plasticized gliadins increased in the blend. As shown in the TGA and DTG curves, the degradation processes occurred separately in the PCL/TPG blends, and the presence of plasticized gliadins only resulted in a slight shifting of the peak signal of neat PCL towards a lower temperature. This observation suggested an immiscible character of the components in the binary blends, as evidenced in the SEM analysis.

Dynamic Mechanical Thermal Analysis

To study the viscoelastic behavior of the films and to determine the glass transition temperature of the samples and its corresponding activation energy, dynamic mechanical analyses were performed in multi-frequency temperature sweep mode from −120 to 50 °C at four different frequencies: 1, 3, 10 and 30 Hz. * MERGEFORMAT Figure 5 shows the evolution with temperature of the storage modulus (*E'*), the loss modulus (*E''*) and the loss factor (tan δ) of PCL and PCL-TPG samples at four tested frequencies. As depicted in the graphs, the storage modulus, which is related with the elastic behavior and stiffness of a certain material, decreased steadily in the temperature range from −120 to −60 °C. Above this temperature, a drastic drop in the storage modulus was observed for all samples. This fall in *E'* from ≈3300 MPa to <900 MPa was related to the transition from a glassy to a rubbery state, i.e., the glass transition temperature of PCL (α relaxation, T_α) [47].

Since this transition occurs in a broad temperature range, the tan δ (ratio of loss to storage moduli) peak criterion was used to determine the T_g of the samples at the different frequencies, and the obtained values are reported in Table 3. It could be observed that the glass transition temperature values increased with the test frequency at a constant heating rate. More specifically, the T_g of PCL shifted from −43.6 °C at 1 Hz to −36.6 °C at 30 Hz. By blending PCL with plasticized gliadins, the same tendency was observed and the T_g values with respect pristine PCL, increased as the content of TPG was higher, suggesting that the presence of gliadins induced some restriction in the polymer chains mobility. For PCL-TPG30 blend, the

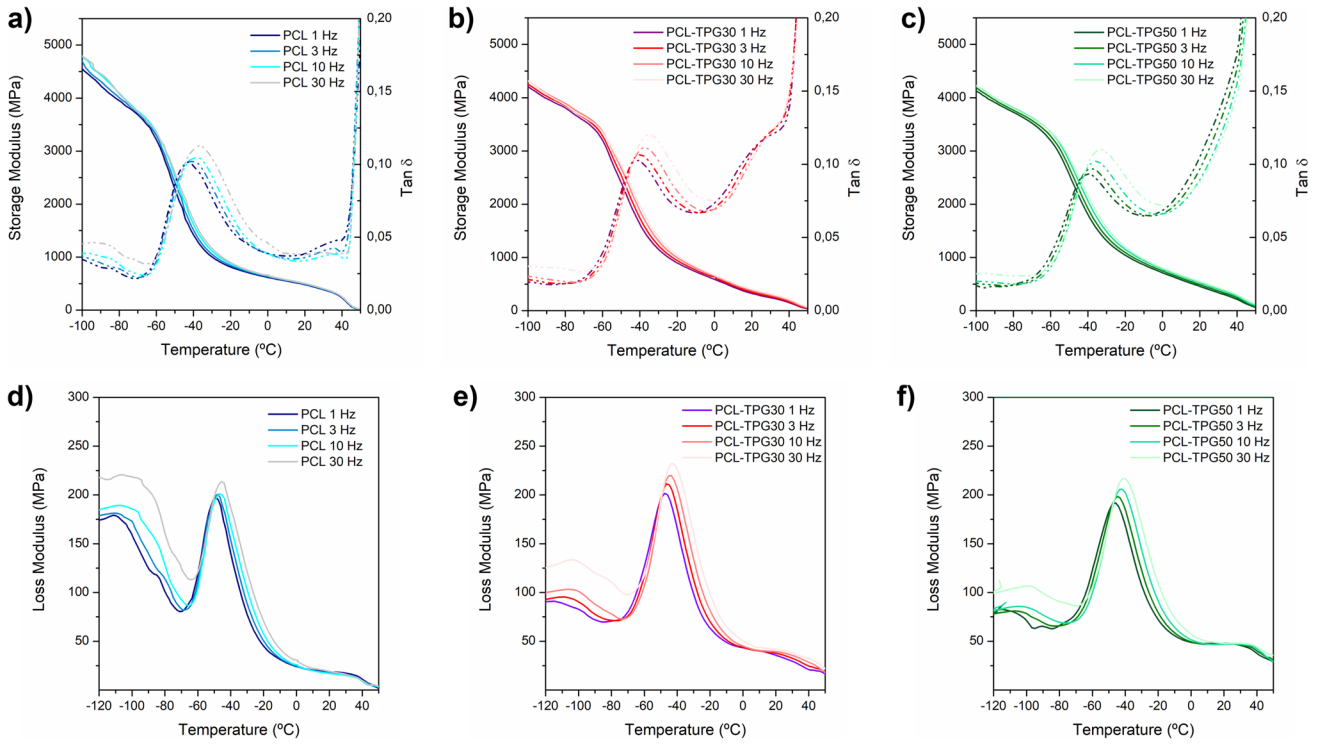

Fig. 5 Temperature dependance of storage modulus (E') and loss factor (tan δ) of (**a**) PCL, (**b**) PCL-TPG30, (**c**) PCL-TPG50 and loss modulus (E'') (***d–f***) at different frequencies (1, 3, 10 and 30 Hz)

Table 3 DMA results of glass transition temperature of samples

	Reference	Frequency (Hz)				Activation energy (kJ mol^{-1})	R^2
		1	3	10	30		
T_α (°C)	PCL	−43.6	−41.3	−38.3	−36.6	212.7	0.987
	PCL-TPG30	−41.5	−39.8	−37.4	−35.1	240.7	0.995
	PCL-TPG50	−40.3	−38.3	−35.8	−33.5	231.8	0.998

tanδ peak shifted from −41.5 °C at 1 Hz to −35.1 °C at 30 Hz, while PCL-TPG50 sample showed a T_g value at 30 Hz of −33.5 °C. For a more in-depth study, the activation energy of the T_g was calculated by using the Arrhenius law, employing the time-temperature superposition principle for the four frequencies investigated. Specifically, the temperature dependance of the test frequency is given by Equation 8 [48]:

$$f = f_0 exp\left(\frac{-E_a}{RT}\right) \tag{8}$$

where R is the gas constant and f and f_0 represent the analogous terms for, respectively, the rate constant and pre-exponential factor in the Arrhenius equation. The variation in glass transition temperature by effect of the test frequency allows the calculation of the activation energy of the glass transition temperature by means of the following equation[48, 49]:

$$E_a = -R\left[\frac{d(lnf)}{d\left(\frac{1}{T_g}\right)}\right] \tag{9}$$

Accordingly, the activation energy of the T_g was obtained by multiplying the slope of the 1/T vs. ln$f$ plot (Figure 6.d) by the gas constant, R = 8.314 ×10^{-3} kJ mol^{-1} K^{-1}and the calculated values are reported in Table 3. The estimated E_a value for PCL was 212.7 kJ mol^{-1}. On the other hand, the addition of gliadins shifted the E_a towards higher values. This increase in the activation energy was in good agreement with the increase in the glass transition temperature in the binary blends of PCL and TPG, since the potential reduction of molecular mobility of polymer chains implies that higher activation energies are required to overcome the softening point of the polymer [50]. In the PCL sample, a plateau was observed following the α-transition, preceding the final decrease in storage and loss modulus as it approached the melting point. Meanwhile, the binary blends of PCL and TPG showed a slight shoulder between 0 °C and 35 °C (as shown in Figure 6b and c), which could be attributed to the presence of an intermediate transition in water or glycerol-plasticized gluten-based materials prior to their characteristic glass transition temperature.[51, 52].

Tensile Properties

The influence of plasticized gliadins over the mechanical performance of PCL films was studied by tensile test. Figure 7 shows the typical stress-strain curves of PCL and PCL/TPG binary blend films while the main mechanical parameters determined from the curves are reported in * MERGEFORMAT Table 4. PCL presented a Young Modulus, a stress at yield and a stress at break of 318 ± 45 MPa, 10.2 ± 1.3 and 31.5 ± 2.9, respectively. This set of films was characterized by a ductile behavior, showing a large plastic deformation before failure at a strain value of 801 ± 78 %. These values are in good agreement with the mechanical parameters reported in previous works for neat PCL [53]. In the stress-strain curve of PCL film, it was possible to observe that after the yield, the stress fell to the draw strength, indicating a necking effect in PCL samples, and remained steady until a strain value around 350 %. From this point, a strain hardening stage provoked by the orientation and alignment of PCL chains was detected owing to its semicrystalline nature. With respect to the binary blend samples, the stress-strain curves showed that the yield point and the elastic modulus decreased as the gliadins content increased.

In a previous work, Finkenstadt et al. reported that filling PCL with wheat gluten (WG) resulted in an increase of the stiffness (Young Modulus) of the samples [16]. The presence of glycerol as plasticizer may explain the reduction of the E in the prepared PCL-TPG blends. This hypothesis is supported by the results reported by Corradini et al., who informed that the elastic modulus did not increase in PCL-zein composites as a consequence of the incorporation of glycerol [14]. PCL-TPG30 also exhibited a strain-hardening behavior but it was not as remarkable as the one observed in pure PCL films, while PCL-TPG50 films showed a little yield, but no evident strain-hardening phenomenon could be noted. Therefore, the stress at break dropped from 31.5 MPa in PCL films to 11.0 and 6.9 MPa in PCL-TPG30 and PCL-TPG50 samples, respectively. Interestingly, PCL-TPG maintained a high flexibility at the two filler contents, 30 and 50 w/w of plasticized gliadins. Specifically, PCL-TPG30 and PCL-TPG50 films showed elongation at break values of 932 ± 92 % and 641 ± 42 %, respectively. The observation of aggregated gliadin particles in SEM analysis that

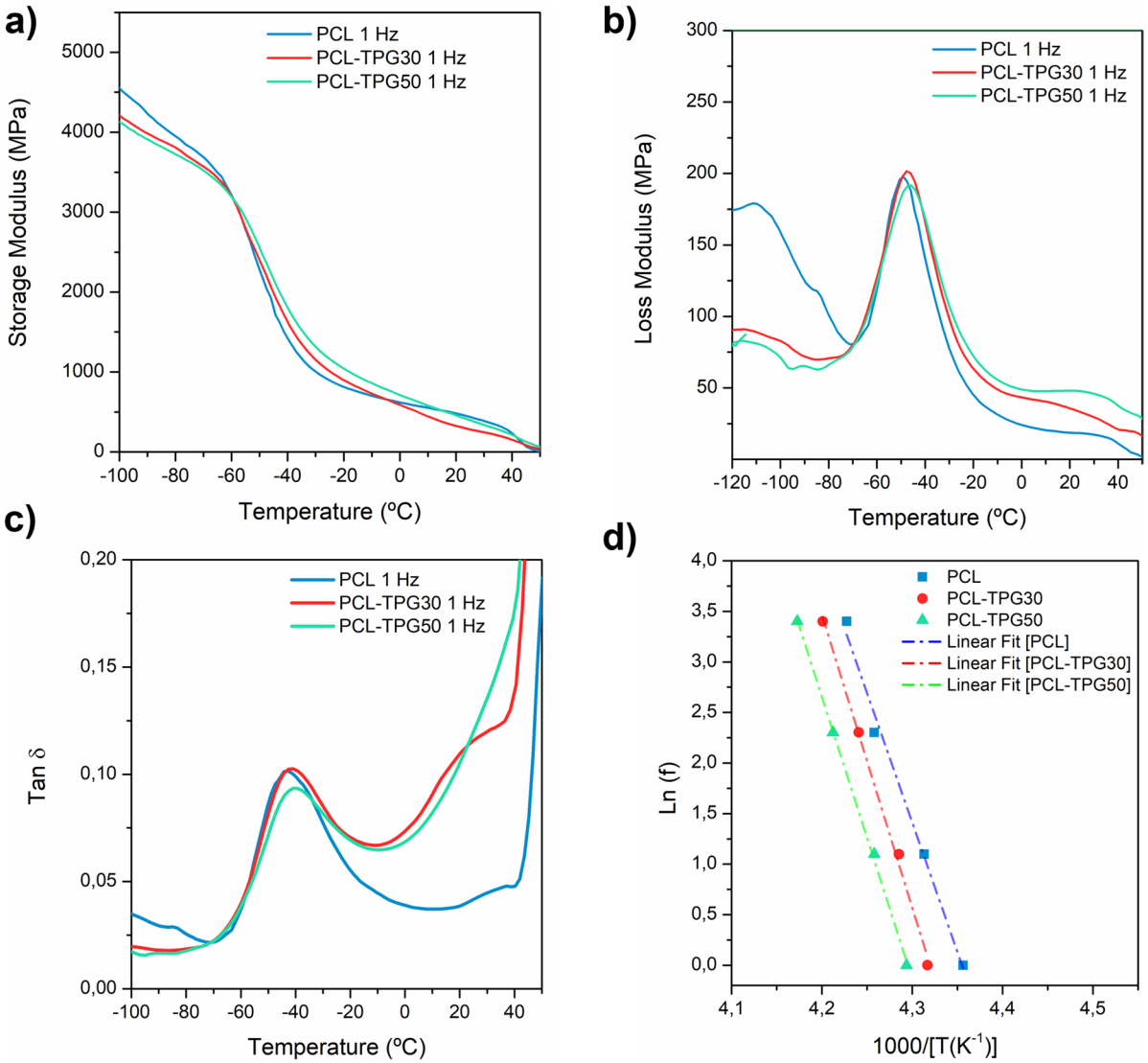

Fig. 6 Thermomechanical behavior of PCL and PCL/TPG blends determined by DMA. **a** Storage modulus, **b** loss modulus and **c** tanδ of films tested at 1 Hz. **d** represents the plot of $1/T_g$ vs. ln*f* based on tanδ peaks

can act potentially as epicenter of defects-formation may explain the reduction in the elongation at break values of PCL-TPG50 film, in which larger conglomerates could be detected.

In the research conducted by Finkenstadt and coworkers, PCL also retained a high flexibility up to 20 % of wheat gluten while from 35 % content of WG, the strain at break dropped drastically to less than 100 % [16]. A similar reduction in elongation values was found for PCL incorporated with other natural materials such as starch, zein and lignin [14, 37, 54, 55]. Thus, the strain at break values reported in our study highlight the positive effect of glycerol and the manufacturing method on the stretchability performance of PCL-TPG films.

Seal Strength

One of the most widely used form of flexible films in food packaging applications is lidding film sealed on e.g., trays or polymer-based container that can seal itself [56, 57]. In this study, the ability of the developed films to seal with themselves was investigated aiming to provide a useful understanding of the peel-seal behavior and the type of peel failure in each case. * MERGEFORMAT Figure 8 gives a visual representation of the type of samples used for carrying out the test in which the sealing zone can be seen while * MERGEFORMAT Table 5 reports the peel strength of the films sealed at different temperatures, maintaining a constant time and pressure (1 second and 0.2 MPa, respectively).

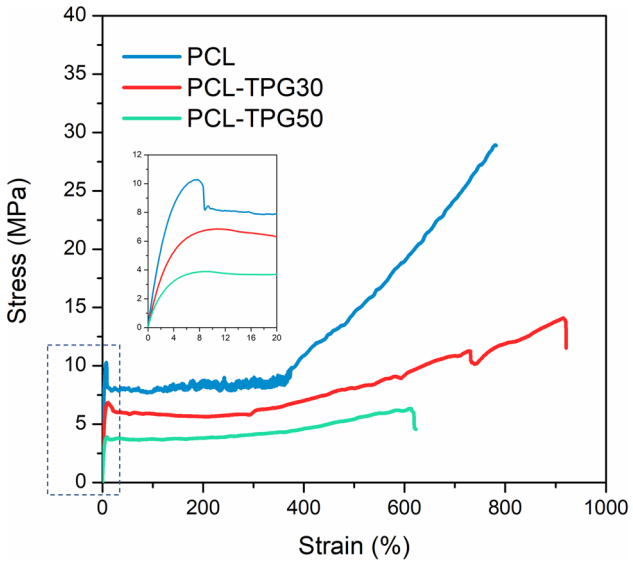

Fig. 7 Representative stress–strain curves of the films

Table 4 Mechanical properties of the developed films determined by tensile test

Reference	E (MPa)	σ_y (MPa)	σ_b (MPa)	ε_b (%)
PCL	318 ± 45	10.2 ± 1.3	31.5 ± 2.9	801 ± 78
PCL-TPG30	199 ± 9	6.7 ± 0.4	11.0 ± 0.5	932 ± 92
PCL-TPG50	155 ± 7	5.3 ± 0.9	6.9 ± 1.5	641 ± 42

At 60 °C, PCL had very low seal strength (0.5 N/15 mm) indicating an adhesive peeling behavior. By applying this temperature, the seal strength gradually increased with increasing the content of plasticized gliadins in the films (2.6 N/15 mm for PCL-TPG30 and 4.6 N/15 mm in the case of PCL-TPG50 film) indicating that the presence of gliadins promoted a stronger interfacial bonding of the films [58]. By varying the sealing temperature to 63 °C, the seal strength increased for the three samples. Specifically, PCL presented a peel strength of 9.8 N/15 mm while the values obtained for PCL-TPG30 and PCL-TPG50 films were 13.2 N/15 mm and 9.1 N/15 mm, respectively. All samples showed a cohesive failure at a sealing temperature of 63 °C, which means that the film tended to peel off and peel continues during the stretching. By applying a seal temperature of 65 °C, the cohesive failure changed to partial tearing in the PCL film while the binary blend formulations still presented a cohesive failure at this temperature. The partial tearing failure consisted of a small peel at the starting and after a certain displacement, the tear of the peel arm occurred [59]. For all references, the average seal strength of films sealed at 65 °C was higher with respect to the values obtained at lower sealing temperatures. The obtained results indicated that the developed materials could have practical properties for peelable film applications, showing peel strengths values between 2.6– 16.2 N/15 mm in the sealing temperature range of 60 –65 °C. In the work conducted by Poisson et al., authors also revealed differences in peel failures upon varying the sealing temperatures of a conventional multilayer film structure consisted of polyethylene/tie-layer/polyamide [56]. They reported that at low sealing temperatures, the film failed due to separation (adhesive), and at high temperatures, the film failed due to tearing (non-peelable). An example with compostable films is provided by Liewchirakorn et al. The authors prepared four different film compositions of polylactic acid (PLA) with poly(butylene adipate-co-terephthalate) (PBAT) through extrusion and revealed that the film composition of PLA/PBAT 80/20, with a thickness of approximately 20 µm, was the most suitable candidate for use as an easy-peel lidding film for a PLA container [59]. They reported peel strengths ranging between 8 and 10 N/15 mm, using a wide range of sealing temperatures (75°C-105°C). Similar values, ranging between 8.4 and 10.0 N/15 mm, were found by Hernandez-García et al., who developed different active starch-polyester bilayer films [58]. Future works in this regard can investigate

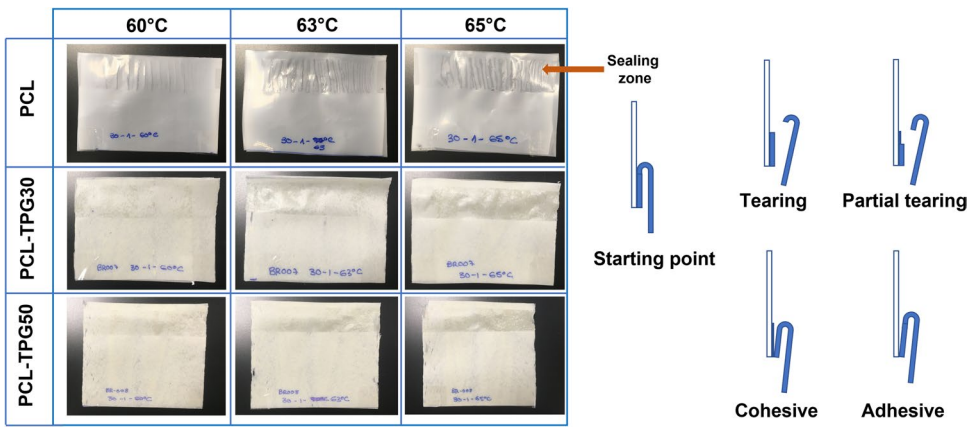

Fig. 8 Illustrative representation of the peel-seal test and typical failure types

Table 5 Peel-strength of the different films sealed at different temperatures

Film	Thickness (μm)	Peel strength (N/15 mm) at different sealing temperatures (°C)		
		60	63	65
PCL	168 ± 2	0.5 ± 0.1	9.8 ± 2.9	13.5 ± 3.7
PCL-TPG30	165 ± 22	2.6 ± 0.8	13.2 ± 6.0	16.2 ± 7.3
PCL-TPG50	213 ± 30	4.6 ± 2.7	9.1 ± 5.0	9.3 ± 4.1

the influence of film thickness on the peel strength of the developed samples since it is reported that film thickness plays a crucial role in the peel seal properties of polymeric substrates [59].

Water Uptake, Contact Angle and Water Vapor Permeability.

The control PCL film and the blend films of PCL/TPG maintained their integrity after being immersed in water for one day, indicating that the compostable films incorporated with plasticized gliadins had a reasonable water resistance after the extrusion process. This observation supports the hypothesis that some cross-linking reactions in gliadin proteins may occur and be favored by the high temperature and the shear stresses during the extrusion process [60, 61]. Nevertheless, films containing plasticized gliadins presented high water absorption capacity, that increased with higher TPG content in the film, while the water uptake of PCL control film could be considered negligible, since it was below 1 %, as reported in Table 6. This result was related to the ability of the hydrophilic groups present in gliadins and glycerol to absorb water.

On the other hand, the surface wettability was determined by calculating the water contact angle (WCA) using a goniometer. PCL showed water contact angles at the initial stage and after 60 seconds of 83.6 ±2.6 ° and 78.9 ±1.7 ° (Figure 9), respectively, being in good agreement with previous data found in literature [62, 63]. Incorporation of plasticized gliadins led to a slight decrease in contact angle in the sample PCL-TPG30 (final contact angle of 70.7 ± 2.7 °), and to a more remarkable decrease with

Table 6 Water uptake (WU) and water vapor permeability of the films

Reference	WU (%)	WVP [(g mm)/(m^2 day mmHg)] @ 23 °C/50% RH
PCL	0.2 ± 0.05	0.33 ± 0.01
PCL-TPG30	8.1 ± 0.9	0.36 ± 0.01
PCL-TPG50	16.3 ± 0.7	0.49 ± 0.03

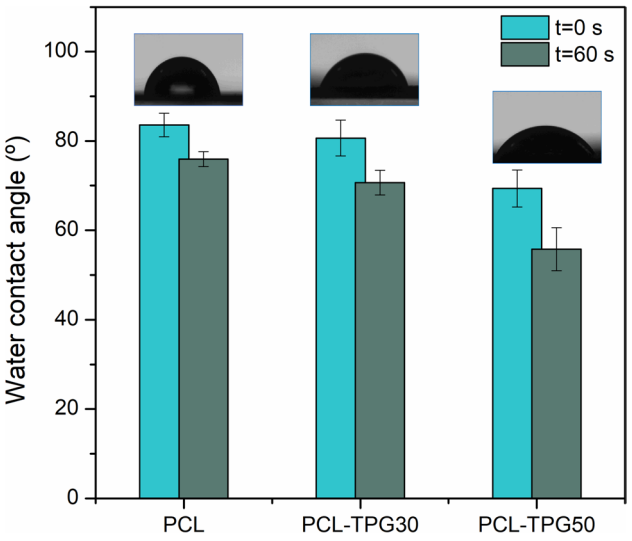

Fig. 9 Water contact angle values for PCL and PCL-TPG films

the addition of 50 wt.% of gliadins, shifting to a contact angle value after 60 seconds of 55.7 ± 4.9 °. The reduction in WCA values was associated with a more water sensitive surface promoted by the presence of hydrophilic amino and −OH groups in gliadins and glycerol, respectively. In addition, physical considerations such as the aspect of the film surface can also impact the wettability of the samples. In this line, PCL showed a smooth surface, as reported in the SEM analysis, while several heterogeneities could be clearly detected along the PCL-TPG films, suggesting that the increase in the hydrophilicity can be also associated with a rougher surface [64].

Water vapor permeability was also measured since it is an important property of films intended for food applications. This process consists of different stages, including the dissolution of water molecules on one side of the film, followed by their diffusion through the film section and lastly, their desorption and evaporation at the other side of the film sample [65]. In this study, the water vapor permeabilities were obtained at 23 °C and at a relative humidity of 50 % and the results are reported in Table 6. The value of water vapor permeability of polycaprolactone film was 0.33 ± 0.01 (g mm)/(m^2 day mmHg). The WVP increased slightly with the incorporation of 30 wt.% of gliadins to a value of 0.36 ± 0.01 (g mm)/(m^2 day mmHg), while blending PCL with up to 50 wt.% of TPG increased the WVP of the film by 48 %. This result was ascribed mainly to the increase in the hydrophilicity of the films owing to the high content of amide groups in gliadins, that can form hydrogen bonds with water molecules [66]. Overall, the developed blends exhibited moderate water vapor permeability. In comparison to other commonly used biodegradable polymers, such as polylactic acid, which typically has a water vapor permeability

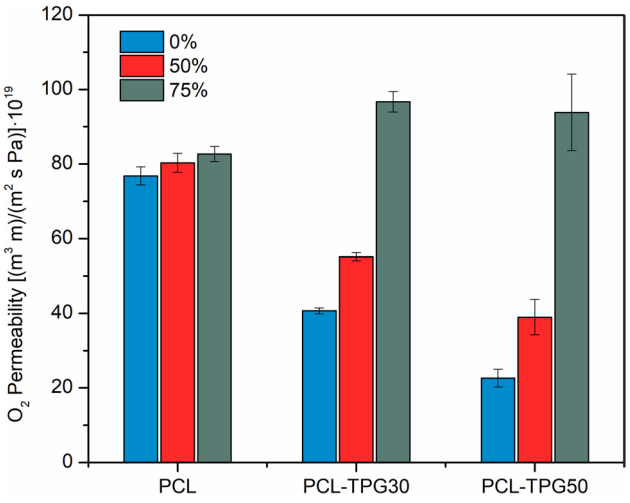

Fig. 10 Oxygen permeability coefficients of PCL and PCL-TPG tested at different RH: 0%, 50% and 75%

around 0.23 (g mm)/(m^2 day mmHg), the PCL-based blends demonstrated slightly higher values [67].

Oxygen Permeability

The coefficients of oxygen permeability calculated at three different relative humidity values: 0 %, 50 % and 75 % at 23 °C are displayed in Figure 10. Relative humidity had a negligible influence in the oxygen permeability of PCL, presenting values in the range of 76.8×10^{-19} to 82.7×10^{-19} (m^3 m)/ (m^2 s Pa), which are close to those found in the literature [68]. On the other hand, gliadins are well known to have very low oxygen permeability coefficients at room temperature and below 50 % relative humidity compared to commodity materials such as polyethylene, polypropylene, or polystyrene [66, 69]. Consequently, extruded films of PCL blended with 30 and 50 wt.% of plasticized gliadins showed a reduction in the O_2 permeability of up to 70 % for the PCL-TPG50 film tested at 0 % RH. For instance, compared to some conventional polymers, PCL-TPG blends appeared to have comparable oxygen barrier properties than polypropylene or polyethylene, which present respective oxygen permeability values in the range of 5.7×10^{-18}—1.2×10^{-17} and 5.7×10^{-18}—2.3×10^{-17} (m^3 m)/ (m^2 s Pa) [68]. However, the permeability values were highly influenced by the relative humidity, and, by increasing the RH to 75 %, the O_2 permeability values were above the one obtained for control PCL film. These results were somehow expected since the higher hydrophilicity of the developed binary blend films reported in previous characterization results, implies a higher amount of sorbed water, which may result in a plasticizing effect that favors the oxygen diffusion through the film [70].

Optical and Color Properties

Due to the relevance of visual aspect of plastic films intended for food applications, the optical and color properties were evaluated. As shown in * MERGEFORMAT Figure 11, all the developed films presented high transparency properties, supported by the fact that the institutional logo could be clearly distinguished through all the film samples.

With regard the color attributes of PCL-based films blended with thermoplastic gliadins, it could be observed that the incorporation of gliadins in the formulation led to a great increase in the *b** parameter (Table 7). This result was consisted with the visual observation and means that the prepared films acquired a yellowish tonality. The coloration was related with the heat-treatment of gliadins during the extrusion process and has been previously observed in wheat gluten-based films [19, 71]. On the other hand, all samples showed high *L** values (>90) indicating a great lightness whereas the *a** parameter shifted to negative values with

Fig. 11 Visual aspect of the developed films

Table 7 Thicknesses of films and color parameters obtained from the CIELab space

Reference	Thickness (μm)	L	a*	b*	ΔE
PCL	168 ± 2	95.7	−0.48	0.96	–
PCL-TPG30	165 ± 22	95.0 ± 0.16	−2.58 ± 0.01	14.63 ± 0.28	13.85 ± 0.29
PCL-TPG50	213 ± 30	94.4 ± 0.04	−2.86 ± 0.06	17.22 ± 0.31	16.49 ± 0.31

the incorporation of gliadins, thus, resulting in a slight green tonality of the PCL-TPG films. These changes were responsible of the total color differences of the PCL-TPG films (13.8 for PCL-TPG30 and 16.5 for PCL-TPG50) with respect to the control PCL film, evidencing that the color variations can be easily noticeable by the human eye.

Home-Compostability Test

Home and community composting is usually referred to the composting of domestic organic waste from kitchens and gardens by households and in many times, it is the most beneficial approach of handling domestic biodegradable waste from the environmental point of view, as it reduces or even eliminates the costs associated with collection and transportation of wastes [72, 73]. According to the hierarchy of aggressiveness for biodegradation environments, home-composting is the second most aggressive one after industrial composting. While industrial composting test is carried out at 58 °C, the home compostability assessment is conducted in the temperature range of 20-30 °C, and, consequently, the type of fungi and bacteria involved in the biodegradation process is different. The biodegradability is an intrinsic property of a certain material and, according to the standard, the percentage of biodegradation should reach at least 90 % with respect to the reference sample (microcrystalline cellulose) in up to 12 months. In contrast, the disintegrability depends on factors such as the dimensions, thickness, or geometry of the finished product, i.e., cast-extruded films in our study. The dry weight of each sample used to conduct the biodegradation test was around 15 grams and the proportion of total organic carbon (grams of C/ grams of dry sample) in plasticized gliadins, PCL, PCL-TPG30 and PCL-TPG50 was, respectively, 40.5 %, 60.2 %, 54.6 % and 51.3 %. Figure 12displays the cumulative biodegradation (%) of microcrystalline cellulose as positive reference sample, plasticized gliadins, polycaprolactone and the blends of PCL and TPG over 210 days of test. According to the standard, the degree of biodegradation of the reference sample must be higher than 70 % after 90 days. As shown, cellulose reached 85 % biodegradation after 85 days of test; therefore, the experimental assay was considered valid. Plasticized gliadins presented a very fast biodegradation profile, reaching a plateau with a maximum of 90 % (110 % with respect to cellulose) just after 60 days. This quick biodegradation profile of gluten-based materials has been also observed in different media by several authors [74–76]. On the other hand, neat PCL showed an initial lag period of 16 days, followed by the

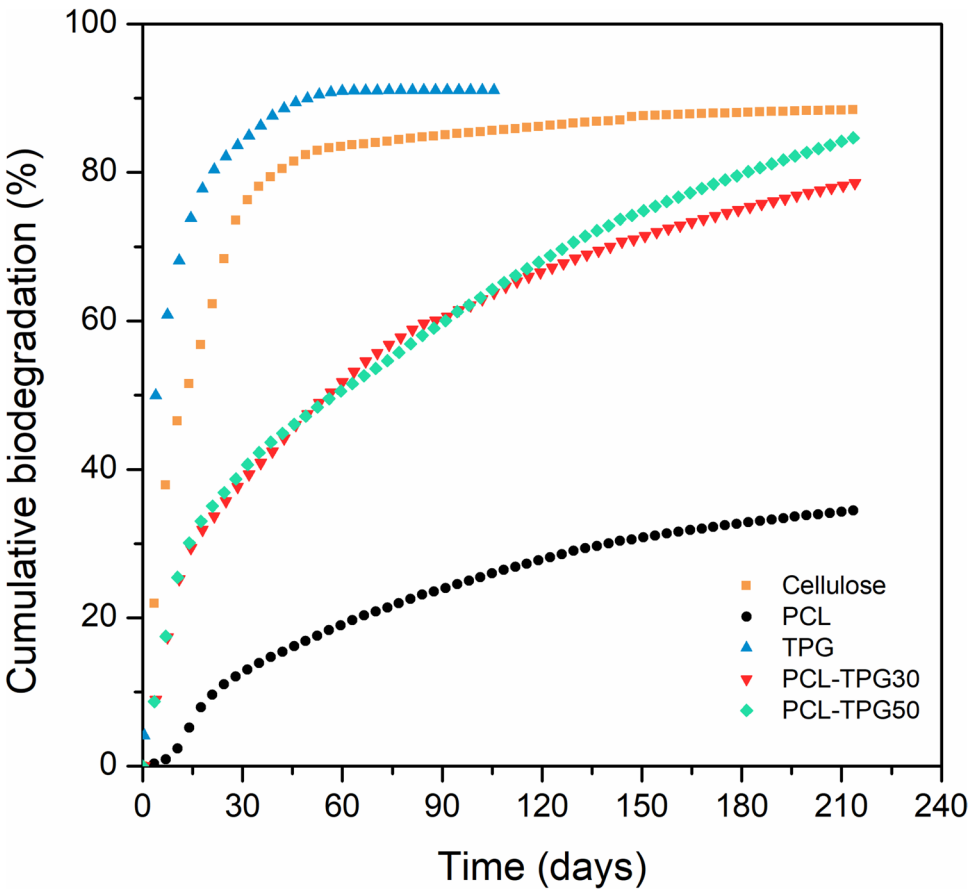

Fig. 12 Cumulative biodegradation of thermoplastic gliadins, PCL, and their blends under home-composting conditions

degradation phase which steadily progressed up to reaching a percentage biodegradation (%B) with respect to MCC of 40 % after 210 days. As the employed grade of PCL used in this work is certified as *home compostable* by TÜV Austria, it implies that the material may take up to 365 days to achieve 90 % biodegradation with respect microcrystalline cellulose. This result contrasted with the fast biodegradation profile observed for PCL under industrial composting conditions carried out at 58 °C in the work conducted by Hong et al. [77]. In this study, carried out at 25 °C, as PCL is not in the molten state, the crystalline parts of PCL could certainly represent an obstacle for enzymes. Finally, the blends of PCL/TPG showed an intermediate biodegradation profile between pure plasticized gliadins and PCL. Although as observed in DSC analysis, gliadins induced a nucleating effect on PCL polymer matrix, with its corresponding increase in the degree of crystallinity, the amorphous nature of gliadin proteins and their easy accessibility to the action of enzymes, led to a faster biodegradation compared to pristine PCL polymer, reaching after 210 days a %B of 89 % and 96 % for PCL-TPG30 and PCL-TPG50, respectively. The faster biodegradation profile of PCL-TPG blends is also supported by previous studies that suggested that an increase in both the hydrophilicity nature of a material or in the surface roughness are factors that promote a faster biodegradation rate [17, 78]. The obtained results evidenced that by varying the content of TPG in the PCL/TPG blends, it was allowed to modulate the biodegradation rate of PCL, which may result interesting in certain applications where a controlled biodegradation process is desired.

The next step of the home compostability assessment was the disintegration test, which was carried out following the French standard NF T 51-800. * MERGEFORMAT Figure 13 shows the qualitative evaluation of the disintegrability of PCL film and the blend films of PCL and plasticized gliadins at different testing times of exposition to the compost medium. It could be observed that after 19 days, the visual aspect of the binary blends changed, with a yellowing effect and a loss of transparency related to changes in the crystallinity of the samples. This observation was explained by a preferential and faster hydrolytic degradation process in the amorphous domains due to the presence of gliadins in the blends [7]. Balaguer et al. reported a complete disintegration of pure gliadin/glycerol films just after 4 days, which was associated with a bulk degradation of the gliadin film coupled with enzymatic cleavage of hydrolyzable amide groups [75]. In the present study, all film samples maintained their integrity after 19 days and the % disintegration of PCL, PCL-TPG30 and PCL-TPG50 films was, respectively, 1 %, 20 %, and 31 %. After 71 days of assay, noticeable changes in the three film samples could be detected. On the one hand, PCL film acquired a brownish tonality, and a loss of transparency was appreciable, indicating the beginning of the hydrolytic degradation of PCL. This process mainly results in small molecules, i.e., water and low molecular weight by-products, that are able to penetrate through the film sample causing chain fragmentations in the matrix and, consequently, a decrease in the average molecular weight of the polymer [79–81]. On the other hand, PCL-TPG films started to break into distinguishable fragments, indicating that the binary blends presented a higher disintegration rate compared to the pristine PCL film. More specifically, the % disintegration at this stage (day 71) of PCL, PCL-TPG30 and PCL-TPG50 films was 12 %, 39 % and 41 %, respectively. On day 120, PCL-TPG films demonstrated a satisfactory complete disintegration since no more than 10 % of their original dry mass remained in the oversized fraction after sieving through a 2 mm sieve, and film residues were

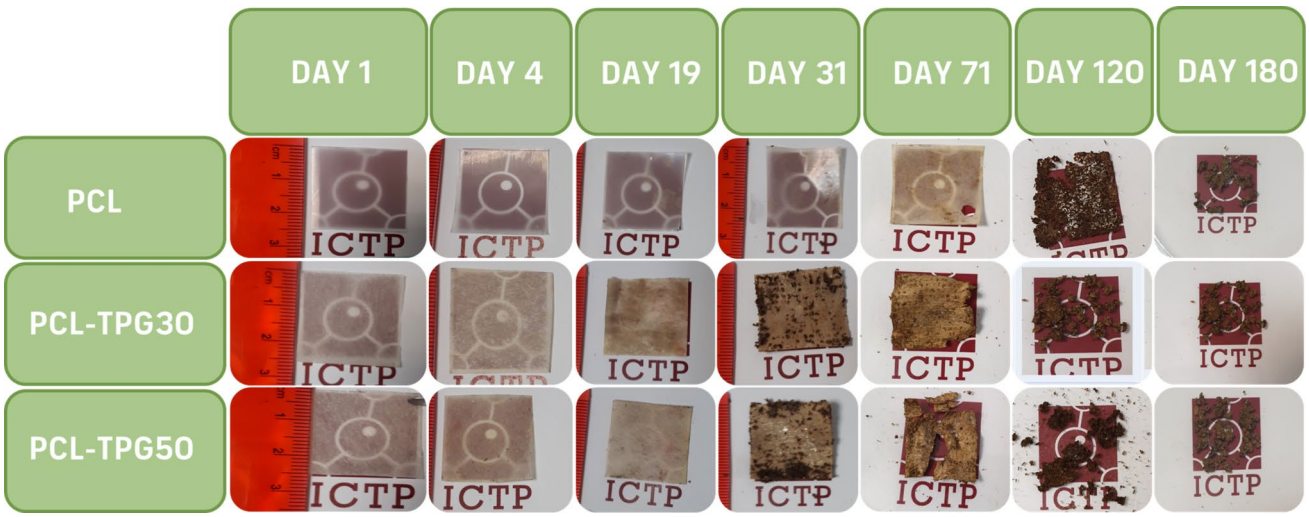

Fig. 13 Photographs taken at different times of the PCL and PCL-TPG films under home-composting conditions

indistinguishable to the naked eye from the other matter in the compost. This result indicated that the presence of gliadins increased the disintegration rate with respect to pristine PCL film, which needed up to 180 days to show a complete disintegration.

Conclusions

In the present study, compostable films based on PCL and thermoplastic gliadins were developed successfully by conventional extrusion transformation process. The addition of gliadins led to a yellow tonality of the films but did not affect the high transparency characteristic of PCL. DSC study revealed a temperature-induced nucleation effect of gliadins over PCL, resulting in an increase in the degree of crystallinity, which shifted from 57 % for PCL to 83 % for PCL-TPG50 sample. Thermogravimetric analysis showed a lower onset degradation temperature of the binary blends with respect to pristine PCL due to the presence of glycerol, which presented a thermal degradation range between 120 and 260 °C while the maximum peak degradation temperature of PCL (T_{max}) was not affected by the incorporation of gliadins. Interestingly, blending PCL with 30 wt.% and 50 wt.% of thermoplastic gliadins did not affect the high flexibility characteristic of PCL-based films, presenting all samples elongation at break values above 600 %, while Young Modulus was seen to decrease with the incorporation of thermoplastic gliadins. The determination of the barrier properties of the films showed that the presence of gliadins significantly reduced the oxygen permeability at 0 % and 50 % relative humidity values while, in contrast, the higher water sensitivity of the films incorporated with gliadins led to an increase of the WVP with respect pure PCL. Finally, the home-compostability assessment showed that gliadins promoted an accelerated aerobic biodegradation and disintegration of the films. Therefore, the materials developed in this work can be considered excellent candidates for sustainable packaging solutions. Furthermore, the presence of a large number of reactive side groups in gliadins can offer an interesting route to prepare packaging films with enhanced functionalities.

Supplementary Information The online version contains supplementary material available at https://doi.org/10.1007/s10924-023-03163-8.

Author Contributions AAG: Data curation, Formal analysis, Investigation, Methodology, Writing—Original draft, Visualization, Writing, Review & Editing. PFMG: Formal analysis, Investigation, Methodology, Writing—Original draft. MG: Funding acquisition, Investigation, Project Administration, Resources, Supervision, Writing, Review & Editing. RG: Conceptualization, Formal analysis, Funding acquisition, Investigation, Project Administration, Resources, Supervision, Validation, Visualization, Writing, Review & Editing. DL: Investigation, Methodology, Validation, Resources, Supervision, Writing, Review & Editing. PHM: Conceptualization, Formal analysis, Funding acquisition, Investigation, Project Administration, Resources, Supervision, Validation, Visualization, Writing, Review & Editing.

Funding The authors would like to express their gratitude to the Generalitat Valenciana (Grant IMAMCA/2022/10) and the Spanish Ministry of Science and Innovation (Grant PID2021-123077OB-I00 funded by MCIN/AEI/10.13039/501100011033 and by the "ERDF A way of making Europe") for their financial support.

Declarations

Competing interests The authors declare no competing interests.

References

1. Beitzen-Heineke EF, Balta-Ozkan N, Reefke H (2017) The prospects of zero-packaging grocery stores to improve the social and environmental impacts of the food supply chain. J Clean Prod 140:1528–1541
2. Gutiérrez Carmona TJ, Alvarez VA (2018) Bionanocomposite films developed from corn starch and natural and modified nanoclays with or without added blueberry extract. Food Hydrocoll 1(77):407–420
3. MacArthur DE, Waughray D, Stuchtey MR (2016) The new plastics economy, rethinking the future of plastics. World Economic Forum. Ellen MacArthur Foundation and McKinsey Company, London
4. Arman Alim AA, Mohammad Shirajuddin SS, Anuar FH (2022) A review of nonbiodegradable and biodegradable composites for food packaging application. J Chem. https://doi.org/10.1155/2022/7670819
5. Popa M, Mitelut A, Niculita P et al (2011) Biodegradable materials for food packaging applications. J Environ Prot Ecol 12:1825–1834
6. Rydz J, Musioł M, Zawidlak-Węgrzyńska B, Sikorska W (2018) Present and future of biodegradable polymers for food packaging applications. Biopolym food Des. https://doi.org/10.1016/B978-0-12-811449-0.00014-1
7. Aragón-gutierrez A, Arrieta MP, López-gonzález M et al (2020) Hybrid biocomposites based on poly (lactic acid) and silica aerogel for food packaging applications. Materials 13(21):4910
8. Thakur M, Majid I, Hussain S, Nanda V (2021) Poly(ε-caprolactone): A potential polymer for biodegradable food packaging applications. Packag Technol Sci 34:449–461. https://doi.org/10.1002/pts.2572
9. Vilaplana F, Strömberg E, Karlsson S (2010) Environmental and resource aspects of sustainable biocomposites. Polym Degrad Stab 95:2147–2161
10. Abdellah Ali SF (2016) Mechanical and thermal properties of promising polymer composites for food packaging applications. IOP Conf Ser Mater Sci Eng. https://doi.org/10.1088/1757-899X/137/1/012035
11. Ilyas RA, Zuhri MYM, Norrrahim MNF et al (2022) Natural Fiber-Reinforced polycaprolactone green and hybrid biocomposites for various advanced applications. Polymers (Basel) 14:1–28. https://doi.org/10.3390/polym14010182
12. Avella M, Errico ME, Laurienzo P et al (2000) Preparation and characterisation of compatibilised polycaprolactone/starch composites. Polymer (Guildf) 41:3875–3881
13. Ramírez-Arreola DE, Robledo-Ortiz JR, Moscoso F et al (2012) Film processability and properties of polycaprolactone/thermoplastic starch blends. J Appl Polym Sci 123:179–190

14. Corradini E, Mattoso LHC, Guedes CGF, Rosa DS (2004) Mechanical, thermal and morphological properties of poly(ε-caprolactone)/zein blends. Polym Adv Technol 15(6):340–345
15. John J, Tang J, Bhattacharya M (1998) Processing of biodegradable blends of wheat gluten and modified polycaprolactone. Polymer (Guildf) 39:2883–2895. https://doi.org/10.1016/S0032-3861(97)00553-3
16. Finkenstadt VL, Mohamed AA, Biresaw G, Willett JL (2008) Mechanical properties of green composites with polycaprolactone and wheat gluten. J Appl Polym Sci 110:2218–2226. https://doi.org/10.1002/app.28446
17. Gutiérrez TJ, Mendieta JR, Ortega-Toro R (2021) In-depth study from gluten/PCL-based food packaging films obtained under reactive extrusion conditions using chrome octanoate as a potential food grade catalyst. Food Hydrocoll. 111:106255. https://doi.org/10.1016/j.foodhyd.2020.106255
18. Hernández-Muñoz P, Kanavouras A, Ng PKW, Gavara R (2003) Development and characterization of biodegradable films made from wheat gluten protein fractions. J Agric Food Chem 51:7647–7654
19. Pau-Balaguer M, Gomez-Estaca J, Gavara R, Hernandez-Munoz P (2011) Functional properties of bioplastics made from wheat gliadins modified with cinnamaldehyde. J Agric Food Chem 59:6689–6695. https://doi.org/10.1021/jf200477a
20. Zhu G, Xu Q, Qin R et al (2005) Effect of γ-radiation on crystallization of polycaprolactone. Radiat Phys Chem 74:42–50
21. ISO 527–3:2018 Plastics (2018) Determination of tensile properties — Part 3: Test conditions for films and sheets
22. ASTM F88 / F88M-15 (2015) Standard Test Method for Seal Strength of Flexible Barrier Materials 1. ASTM Int. 1–11
23. Kormin S, Kormin F, Beg MDH (2019) Study on the biodegradability and water adsorption of ldpe/sago starch blend. In: Journal of Physics: Conference Series. IOP Publishing p 12033
24. ASTM D3985 - 17 (2017) Standard Test Method for Oxygen Gas Transmission Rate Through Plastic Film and Sheeting Using a Coulometric Sensor. In: ASTM annual book of standards
25. ASTM F1927-20 (2020) Standard Test Method for Determination of Oxygen Gas Transmission Rate , Permeability and Permeance at Controlled Relative Humidity Through Barrier Materials Using a Coulometric Detector. 1–6
26. ASTM F1249-20 (2020) Standard Test Method for Water Vapor Transmission Rate Through Plastic Film and Sheeting Using a Modulated Infrared Sensor. ASTM Int.
27. NF T51-800 (2015) Plastics - Specifications for plastics suitable for home composting
28. UNE-EN ISO 14855–1:2013 (2013) Determinación de la biodegradabilidad aeróbica final de materiales plásticos en condiciones de compostaje controladas. Método según el análisis de dióxido de carbono generado. Parte 1: Método general.
29. ISO 20200:2015 Plastics (2015) Determination of the degree of disintegration of plastic materials under simulated composting conditions in a laboratory-scale test. 1–8
30. Zárate-Ramírez LS, Martínez I, Romero A et al (2011) Wheat gluten-based materials plasticised with glycerol and water by thermoplastic mixing and thermomoulding. J Sci Food Agric 91:625–633. https://doi.org/10.1002/jsfa.4224
31. Balaguer MP, Gomez-Estaca J, Cerisuelo JP et al (2014) Effect of thermo-pressing temperature on the functional properties of bioplastics made from a renewable wheat gliadin resin. LWT—Food Sci Technol 56(1):161–167. https://doi.org/10.1016/j.lwt.2013.10.035
32. Dhaka V, Khatkar BS (2016) Microstructural, thermal and IR spectroscopy characterisation of wheat gluten and its sub fractions. J Food Sci Technol 53:3356–3363. https://doi.org/10.1007/s13197-016-2314-9
33. Flores-Cedillo ML, Alvarado-Estrada KN, Pozos-Guillén AJ et al (2016) Multiwall carbon nanotubes/polycaprolactone scaffolds seeded with human dental pulp stem cells for bone tissue regeneration. J Mater Sci Mater Med 27:1–12. https://doi.org/10.1007/s10856-015-5640-y
34. Huang A, Jiang Y, Napiwocki B et al (2017) Fabrication of poly(ε-caprolactone) tissue engineering scaffolds with fibrillated and interconnected pores utilizing microcellular injection molding and polymer leaching. RSC Adv 7:43432–43444. https://doi.org/10.1039/c7ra06987a
35. Diken ME, Koçer Kizilduman B, Doğan S, Doğan M (2022) Antibacterial and antioxidant phenolic compounds loaded PCL biocomposites for active food packaging application. J Appl Polym Sci. https://doi.org/10.1002/app.52423
36. Nashchekina Y, Chabina A, Nashchekin A, Mikhailova N (2020) Different conditions for the modification of polycaprolactone films with l-arginine. Int J Mol Sci 21:1–13. https://doi.org/10.3390/ijms21196989
37. Ortega-Toro R, Contreras J, Talens P, Chiralt A (2015) Physical and structural properties and thermal behaviour of starch-poly(ε{open}-caprolactone) blend films for food packaging. Food Packag Shelf Life 5:10–20. https://doi.org/10.1016/j.fpsl.2015.04.001
38. Ansorena MR, Zubeldía F, Marcovich NE (2016) Active wheat gluten films obtained by thermoplastic processing. Lwt 69:47–54. https://doi.org/10.1016/j.lwt.2016.01.020
39. Noel TR, Parker R, Ring SG, Tatham AS (1995) The glass-transition behaviour of wheat gluten proteins. Int J Biol Macromol 17:81–85. https://doi.org/10.1016/0141-8130(95)93521-x
40. Pouplin M, Redl A, Gontard N (1999) Glass transition of wheat gluten plasticized with water, glycerol, or sorbitol. J Agric Food Chem 47:538–543. https://doi.org/10.1021/jf980697w
41. Laoutid F, Lenoir H, Santaeularia AM et al (2022) Impact-resistant poly(3-Hydroxybutyrate)/Poly(ε -Caprolactone)-based materials, through reactive melt processing, for compression-molding and 3d-printing applications. Mater 15(22):8233
42. Cyras VP, Vázquez A, Kenny JM (2001) Crystallization kinetics by differential scanning calorimetry for PCL/starch and their reinforced sisal fiber composites. Polym Eng Sci 41(9):1521–1528. https://doi.org/10.1002/pen.10851
43. Merino D, Alvarez VA, Pérez CJ (2018) Non-isothermal crystallization of poly(ε-caprolactone) nanocomposites with soy lecithin-modified bentonite. Polym Cryst 3(1):e10020. https://doi.org/10.1002/pcr2.10020
44. Aoyagi Y, Yamashita K, Doi Y (2002) Thermal degradation of poly[(R)-3-hydroxybutyrate], poly[ε-caprolactone], and poly[(S)-lactide]. Polym Degrad Stab 76:53–59. https://doi.org/10.1016/S0141-3910(01)00265-8
45. Mina Hernandez JH (2020) Effect of the incorporation of polycaprolactone (PCL) on the retrogradation of binary blends with cassava thermoplastic starch (TPS). Polymers (Basel) 13(1):38. https://doi.org/10.3390/polym13010038
46. Li M, Yue Q, Liu C et al (2020) Effect of gliadin/glutenin ratio on pasting, thermal, and structural properties of wheat starch. J Cereal Sci 93:102973. https://doi.org/10.1016/j.jcs.2020.102973
47. Feijoo P, Mohanty AK, Rodriguez-Uribe A et al (2022) Biodegradable blends from bacterial biopolyester PHBV and bio-based PBSA: Study of the effect of chain extender on the thermal, mechanical and morphological properties. Int J Biol Macromol. https://doi.org/10.1016/j.ijbiomac.2022.11.188
48. Li G, Lee-Sullivan P, Thring R (2000) Determination of activation energy for glass transition of an epoxy adhesive using dynamic mechanical analysis. J Therm Anal Calorim - J THERM ANAL CALORIM 60:377–390. https://doi.org/10.1023/A:1010120921582

49. Ward I, Sweeney J (2004) An Introduction to The Mechanical Properties of Solid Polymers. Wiley, Hoboken
50. Sonseca A, Salim M, Muñoz-Bonilla A et al (2020) Biodegradable and antimicrobial PLA–OLA blends containing chitosan-mediated silver nanoparticles with shape memory properties for potential medical applications. Nanomater 10:1065. https://doi.org/10.3390/nano10061065
51. Duval A, Molina-Boisseau S, Chirat C, Morel M-H (2016) Dynamic mechanical analysis of the multiple glass transitions of plasticized wheat gluten biopolymer. J Appl Polym Sci. https://doi.org/10.1002/app.43254
52. Sun S, Song Y, Zheng Q (2007) Morphologies and properties of thermo-molded biodegradable plastics based on glycerol-plasticized wheat gluten. Food Hydrocoll 21(7):1005–1013. https://doi.org/10.1016/j.foodhyd.2006.03.004
53. Mahieu A, Terrié C, Agoulon A et al (2013) Thermoplastic starch and poly(ε-caprolactone) blends: Morphology and mechanical properties as a function of relative humidity. J Polym Res. https://doi.org/10.1007/s10965-013-0229-y
54. Abdellah S (2016) Mechanical and thermal properties of promising polymer composites for food packaging applications. IOP Conf Ser Mater Sci Eng 137:12035. https://doi.org/10.1088/1757-899X/137/1/012035
55. Pucciariello R, D'Auria M, Villani V et al (2010) Lignin/Poly(e-Caprolactone) blends with tuneable mechanical properties prepared by high energy ball-milling. J Polym Environ 18:326. https://doi.org/10.1007/s10924-010-0212-1
56. Poisson C, Hervais V, Lacrampe MF, Krawczak P (2006) Optimization of PE/Binder/PA extrusion blow-molded films. I. Heat sealing ability improvement using PE/EVA blends. J Appl Polym Sci 99(33):974–985. https://doi.org/10.1002/app.22405
57. Yousefzadeh Tabasi R, Najarzadeh Z, Ajji A (2015) Development of high performance sealable films based on biodegradable/compostable blends. Ind Crops Prod 72:206–213. https://doi.org/10.1016/j.indcrop.2014.11.021
58. Hernandez García E, Vargas M, Chiralt A (2022) Active starch-polyester bilayer films with surface-Incorporated ferulic acid. Membranes (Basel). https://doi.org/10.3390/membranes12100976
59. Liewchirakorn P, Aht-Ong D, Chinsirikul W (2018) Practical approach in developing desirable peel-seal and clear lidding films based on poly(lactic acid) and poly(butylene adipate-co-terephthalate) blends. Packag Technol Sci 31(5):296–309. https://doi.org/10.1002/pts.2321
60. Lagrain B, Goderis B, Brijs K, Delcour JA (2010) Molecular basis of processing wheat gluten toward biobased materials. Biomacromol 11:533–541. https://doi.org/10.1021/bm100008p
61. Domenek S, Morel M-H, Bonicel J, Guilbert S (2002) Polymerization kinetics of wheat gluten upon thermosetting. A mechanistic model. J Agric Food Chem 50:5947–5954. https://doi.org/10.1021/jf0256283
62. Xin Y-Z, Quan M, Kim S-S et al (2015) Fabrication of MgCl2/PCL Composite Scaffolds Using 3D Bio Plotting System for Bone Regeneration. J Biomater Tissue Eng 5:849–856. https://doi.org/10.1166/jbt.2015.1374
63. Leszczak V, Baskett DA, Popat KC (2014) Smooth muscle cell functionality on collagen immobilized polycaprolactone nanowire surfaces. J Funct Biomater 5:58–77. https://doi.org/10.3390/jfb5020058
64. Herniou–Julien C, Mendieta JR, Gutiérrez TJ (2019) Characterization of biodegradable/non-compostable films made from cellulose acetate/corn starch blends processed under reactive extrusion conditions. Food Hydrocoll. https://doi.org/10.1016/j.foodhyd.2018.10.024
65. Kester JJ, Fennema OR (1986) Edible films and coatings: a review. Food Technol 40:47–59
66. Balaguer MP, Cerisuelo JP, Gavara R, Hernandez-Muñoz P (2013) Mass transport properties of gliadin films: Effect of cross-linking degree, relative humidity, and temperature. J Memb Sci 428:380–392. https://doi.org/10.1016/j.memsci.2012.10.022
67. Carosio F, Colonna S, Fina A et al (2014) Efficient gas and water vapor barrier properties of thin poly(lactic acid) packaging films: functionalization with moisture resistant nafion and clay multilayers. Chem Mater 26:5459–5466. https://doi.org/10.1021/cm501359e
68. Nanni G, Heredia-Guerrero JA, Paul UC et al (2019) Poly(furfuryl alcohol)-polycaprolactone blends. Polymers (Basel). https://doi.org/10.3390/polym11061069
69. Gontard N, Thibault R, Cuq B, Guilbert S (1996) Influence of Relative Humidity and Film Composition on Oxygen and Carbon Dioxide Permeabilities of Edible Films. J Agric Food Chem 44:1064–1069. https://doi.org/10.1021/jf9504327
70. López-de-Dicastillo C, Gómez-Estaca J, Catalá R et al (2012) Active antioxidant packaging films: Development and effect on lipid stability of brined sardines. Food Chem 131(4):1376–1384. https://doi.org/10.1016/j.foodchem.2011.10.002
71. Roy S, Weller CL, Gennadios A et al (1999) Physical and molecular properties of wheat gluten films cast from heated film-forming solutions. J Food Sci 64(1):57–60. https://doi.org/10.1111/j.1365-2621.1999.tb09860.x
72. Adhikari B, Tremier A, Martinez J, Barrington S (2010) Home and community composting for on-site treatment of urban organic waste: Perspective for Europe and Canada. Waste Manag Res 28:1039–1053. https://doi.org/10.1177/0734242X10373801
73. Darwin SEC (2008) Green paper on the management of bio-waste in the European Union. SEC Eur Comm 2936
74. Chevillard A, Angellier-Coussy H, Cuq B et al (2011) How the biodegradability of wheat gluten-based agromaterial can be modulated by adding nanoclays. Polym Degrad Stab 96(12):2088–2097. https://doi.org/10.1016/j.polymdegradstab.2011.09.024
75. Balaguer MP, Villanova J, Cesar G et al (2015) Compostable properties of antimicrobial bioplastics based on cinnamaldehyde cross-linked gliadins. Chem Eng J 262:447–455. https://doi.org/10.1016/j.cej.2014.09.099
76. Zhang X, Gozukara Y, Sangwan P et al (2010) Biodegradation of chemically modified wheat gluten-based natural polymer materials. Polym Degrad Stab 95:2309–2317. https://doi.org/10.1016/j.polymdegradstab.2010.09.001
77. Hong S, Choi W, Cho S et al (2009) Mechanical properties and biodegradability of poly-3-caprolactone/soy protein isolate blends compatibilized by coconut oil. Polym Degrad Stab - POLYM Degrad STABIL 94:1876–1881. https://doi.org/10.1016/j.polymdegradstab.2009.04.029
78. Borghesi D, Molina M, Guerra M, Campos M (2016) Biodegradation study of a novel poly-caprolactone-coffee husk composite film. Mater Res. https://doi.org/10.1590/1980-5373-MR-2015-0586
79. Su S, Kopitzky R, Tolga S, Kabasci S (2019) Polymers review polylactide (PLA) and its blends with poly(butylene succinate) (PBS): A brief review. Polymers (Basel) 11:1193. https://doi.org/10.3390/polym11071193
80. Ramos M, Fortunati E, Beltrán A et al (2020) Controlled release, disintegration, antioxidant, and antimicrobial properties of poly (lactic acid)/thymol/nanoclay composites. Polymers (Basel) 12(9):1878. https://doi.org/10.3390/polym12091878
81. Kalita NK, Bhasney SM, Mudenur C et al (2020) End-of-life evaluation and biodegradation of Poly(lactic acid) (PLA)/Polycaprolactone (PCL)/Microcrystalline cellulose (MCC)

polyblends under composting conditions. Chemosphere 247:125875. https://doi.org/10.1016/j.chemosphere.2020.125875